doi.org/10.36721/PJPS.2024.37.5.REG.981-991.1

Hydroxychloroquine inhibits the growth of lung cancer cells by inducing G1 cell cycle arrest and apoptosis

Shuang Fu[1], Likun Liu[2], Yaoyao Wang[3], Wenlu Liu[1], Siyu Sun[3], Xiu li Gao[2], Wenbin Zhu[2] and Liling Yue[2]*

[1]College of Pharmacy, Qiqihar Medical University, Qiqihar, China,
[2]Research Institute of Medicine and Pharmacy, Qiqihar Medical University, Qiqihar, China,
[3]Department of Medical Technology, Qiqihar Medical University, Qiqihar, China

Abstract: Hydroxychloroquine, used initially as an anti-malarial drug, is now recognized for its anti-tumor effects in a range of human cancers. Nevertheless, there has been limited attention given to the molecular mechanisms of anti-tumor action of hydroxychloroquine. Here, we investigated the anti-tumor effect of hydroxychloroquine in human A549 cells and further analyzed the potential molecular mechanisms involved. Hydroxychloroquine was found to effectively inhibit the growth of A549 cells. This inhibition was observed to be both dose-dependent and time-dependent. Moreover, in a tumor xenograft mouse model, hydroxychloroquine remarkably suppressed tumor growth. Mechanistically, treatment with hydroxychloroquine led to the inhibition of phosphorylation in JNK, STAT3 and AKT. This biochemical interference subsequently induced G1 cell cycle arrest and promoted mitochondrial-mediated apoptosis in A549 cells. The findings from this study offered robust evidence supporting the use of hydroxychloroquine as a treatment for non-small cell lung cancer (NSCLC). Consequently, hydroxychloroquine emerges as a potential therapeutic agent for the treatment of this cancer.

Keywords: Hydroxychloroquine; A549 cell; antitumor action; G1 phase arrest; apoptosis.

Submitted on 15-03-2024 – Revised on 25-6-2024 – Accepted on 19-8-2024

INTRODUCTION

Lung cancer, known as the prevailing malignancy diagnosed universally and the primary contributor to cancer-associated mortality on a global scale, poses a significant public health challenge. Despite advances in treatment modalities, the burden of this disease remains substantial. In addition to its devastating toll on individuals and families, lung cancer exerts a significant economic impact, straining healthcare systems and resources. Garnered an estimated count of approximately 2.5 million fresh incidences and accounted for 1.8 million fatalities in 2022 (Bray *et al.*, 2024). NSCLC, representing the predominant subtype within the spectrum of lung malignancies, encompasses approximately 80-85% of all instances, this type of lung cancer represents the vast majority of total lung cancer occurrences (Guo *et al.*, 2022). Across the span of the last twenty years, notable advancements have been made in both the diagnosis and therapeutic interventions targeting NSCLC. Nevertheless, NSCLC remains a formidable challenge in clinical practice. The metastatic subtype, in particular, poses a huge obstacle and overall prognosis and survival remain low (Herbst, Morgensztern, Boshoff, 2018). A mere 26% of patients diagnosed with NSCLC manage to survive beyond the 5-year mark (Miller, 2022). Tumor recurrence, chemotherapy resistance and metastasis continue to present formidable hurdles in the management of NSCLC, emphasizing the critical need for innovative treatment approaches. Emerging strategies such as immunotherapy and precision medicine offer promising avenues for improving outcomes in NSCLC patients. However, challenges persist in identifying biomarkers predictive of treatment response and overcoming resistance mechanisms. In order to confront these obstacles head-on and improve treatment outcomes for patients, it is imperative to maintain an unwavering commitment to ongoing, exhaustive research endeavors focused on the development of novel pharmaceuticals and synergistic combination therapies. Multidisciplinary collaboration among clinicians, researchers and healthcare policymakers is paramount to advancing the field and ultimately enhancing the lives of individuals affected by NSCLC. As research continues to unravel the complexities of NSCLC biology and therapeutic resistance mechanisms, a concerted effort is needed to translate these discoveries into clinical practice.

Drug repurposing, also referred to as drug rediscovery or drug repositioning, is an appealing strategy that holds the potential to address unmet medical needs in the field of oncology. Compared with traditional drug discovery methods, it offers advantages such as shorter timelines, reduced costs and lower failure rates (Fong, To, 2021). Hydroxychloroquine (HCQ) is an older drug that obtained consent from the US Food and Drug Administration in 1955, marking its entrance into the medical arena. It was originally used for malaria treatment with similar actions to chloroquine (CQ) (Hoekenga, 1955). As a result, it has rapidly gained acceptance. Afterwards, it was found that

**Corresponding authors:* e-mails: zhuwenbin1773@sina.com

the accident finding uncovered its anti-inflammatory properties. As a result, the repurposing of this medication has led to its application in treating autoimmune conditions. Notably, it has shown effectiveness in managing diseases such as rheumatoid arthritis (Ponticelli, Moroni, 2017; Nirk, Reggiori, Mauthe, 2020). Recently, HCQ has garnered increasing attention due to its potential anticancer properties as either a monotherapy or adjuvant therapy for various cancers. Mechanically, HCQ primarily impacts cancer progression by inhibiting autophagy. As a monotherapy, HCQ has exhibited efficacy in restraining the invasion of bladder cancer cells by directly impeding the autophagic flux (Chou *et al*., 2021). Furthermore, research has unveiled that HCQ induces apoptosis reliant on autophagy in cholangiocarcinoma cells. This induction is facilitated by the augmentation of ROS accumulation (Chen *et al*., 2021). In adjuvant therapy, HCQ was discovered to enhance the anti-tumor consequences of bevacizumab (BEV) on glioblastoma (GBM) by inhibiting autophagy (Liu *et al*., 2019). Furthermore, In addition, it was observed that treatment of Lkb1-deficient, Kras-driven lung tumors had a significant effect when autophagy was inhibited using HCQ. Combining HCQ-induced autophagy inhibition with MEK inhibitors has potential therapeutic advantages in protocols for the treatment of these particular lung tumors (Bhatt *et al*., 2023). Apart from its autophagy-related actions, HCQ also exhibits antitumor efficacy through other mechanisms. it can regulate the Bax/Bcl-2 ratio and activate caspase-3, leading to apoptosis in CLL and B-cell CLL (Lagneaux *et al*., 2001; Lagneaux *et al*., 2002). HCQ's impact on human breast cancer cells involves influencing the acetylation status (Rahim, Strobl, 2009), while in NSCLC, it disrupts lysosomal pH and promoting the shift from immunosuppressive M2-like macrophages to pro-inflammatory M1-like ones, thereby activating CD8+ T cell-mediated antitumor immune responses (Li *et al*., 2018). Furthermore, HCQ, in combination with the pan-PI3K inhibitor BKM120, has been shown synergistically induced DNA damage and subsequent cancer cell apoptosis (Peng *et al*., 2021). Given the emerging evidence of HCQ's antitumor effects, further exploration of its pharmacological mechanisms of action is warranted. A comprehensive elucidation of HCQ's multifaceted actions holds significant promise for the advancement of novel anticancer interventions.

This study sets out to delve into the effects of HCQ on NSCLC proliferation and to conduct an initial investigation into the plausible mechanisms underlying its action. In order to do this, A549 cells were exposed to varying concentrations of HCQ treatment. We evaluated the role of HCQ in cell growth, including its effects on cell viability, cell cycle progression, apoptosis, as well as its influence on the amounts of phosphorylation of JNK, STATs, AKT and so on. Furthermore, we looked at how HCQ affected tumor growth using an NSCLC xenograft mouse model. Our discoveries hold the potential to provide invaluable insights into the pharmacological impact of HCQ while addressing NSCLC.

MATERIALS AND METHODS

Reagents and antibodies

HCQ procurement was conducted through Sigma Chemical Co. (St. Louis, MO, USA). Methylthiazol tetrazolium (MTT) acquisition was facilitated through Beyotime Biotech. Inc (Shanghai, China). Dimethylsulfoxide (DMSO) procurement was conducted through Damao chemical reagent factory (Tianjin, China). AO/EB staining Kit acquisition was facilitated through Sangon Biotech Co., Ltd (Shanghai, China). Annexin V-FITC/PI kit procurement was conducted through KeyGEN Bio Tech co., ltd (Nanjing, China). The procurement of BALB/c nude mice, around 5 to 6 weeks old, was conducted through Liaoning Changsheng Biotechnology co., Ltd. (Benxi, China). The antibodies employed in the study were sourced as listed below: GAPDH (2118), Cyclin E1 (20808), CDK2 (2546), Cyclin D1 (2922), CDK4 (12790), p21 (2947), Bcl-2 (2872), Bax (2772), cytochrome C (11940), Caspase-3 (14220), and Poly-ADP-ribose polymerase (9542), p-JNK (4668), JNK (9252), p-STAT3 (52075), STAT3 (12640), p-AKT (4060), AKT (9272), p53 (2527) and anti-rabbit IgG, HRP-linked antibody (7074), all of which are from Cell Signaling Technology.

Cell culture

The procurement process for human lung cancer A549 cells involved coordination with the National Collection of Authenticated Cell cultures (Shanghai, China). These cells were meticulously maintained in a controlled environment, upheld at a constant temperature of 37°C and exposed to a humidified atmosphere, the CO_2 concentration was meticulously maintained at 5%. The culture medium employed for cell growth and maintenance comprised DMEM/F12 medium sourced from Pricella, Wuhan, supplemented with 10% FBS from the same supplier. Additionally, to prevent microbial contamination, a Penicillin-Streptomycin solution, diluted at a ratio of 1:100, sourced from Pricella, Wuhan, was also incorporated into the culture medium.

MTT assay

In this test, the MTT method was utilized to achieve impact of HCQ detection as follows. Initially, following seeding, cells were distributed into individual wells of a 96-well plate, each well accommodating a concentration of 5×10^3 cells. Subsequently, a 24h incubation period was allotted to facilitate cell adhesion and stabilization within the plate environment. Subsequently, the cells received treatment with HCQ, with concentrations ranging between 7.5 and 150μM. This treatment regimen was administered for either 24h or 48h, as per experimental

protocol. Following the respective incubation periods, a 20µl faliquot was drawn from the MTT stock solution, which had a concentration of 5mg/ml, was meticulously dispensed into every individual well. Following this addition, the plate underwent an additional incubation period of 4 hours, maintaining a constant temperature of 37°C. Subsequently, the supernatant was carefully removed. The formazan crystals that remained were then dissolved in 150µl of DMSO. MTT formazan quantified via OD value at 570 nm utilizing Safire2 instrument.

Cell cycle analysis

For the investigation of HCQ's impact on the cell cycle, into individual wells of 6-well plates, A549 cells were inoculated (5×10^4 cells per well) and kept in an incubator set to 37°C for a period of 24 hours. Following incubation, HCQ was added to achieve final concentrations of 30, 60 and 90µM. Cells underwent another 24h incubation at 37°C. Subsequently, the cells were harvested and subjected to fixation with cold 70% ethanol and left to incubate overnight. This incubation took place at a temperature of -20°C. Following centrifugation, the cell pellets underwent staining with propidium iodide (PI) in a light-shielded environment, lasting for a duration of 30 min. This incubation occurred at the prevailing ambient temperature. Data acquisition and subsequent analysis were conducted utilizing the BD FACS Calibur Flow Cytometer.

AO/EB dual staining

To examine the morphological alterations indicative of apoptosis in A549 cells, AO/EB dual staining was conducted. Approximately, into each well of 6-well plates, a population of 5×10^4 cells was introduced for seeding, and allowed to incubate with 24h. Following the incubation, cells underwent treatment with varying concentrations (30, 60 and 90µM) of HCQ for an extra 24h period. Subsequently, AO/EB dye mixture with 100µg/ml of each, ready in PBS, was introduced to the cells for staining purposes. Staining process lasted 15 min at ambient temperature. Finally, morphological observations were conducted utilizing a fluorescence microscope. Untreated cells served as the negative control for comparison.

Annexin V-FITC/PI assay

To assess the biochemical changes associated with apoptosis induced by HCQ, following the manufacturer's instructions, the Annexin V-FITC/PI kit was utilized for the procedure. Briefly, 5×10^4 cells in the exponential phase were seeded into individual wells of 6-well plates. It was left to incubate for 24 h. Subsequently, HCQ was then added to achieve final concentrations ranging ranging between 0 and 90µM. After a further 24h incubation, all cellular specimens were collected and suspended anew in Annexin binding buffer. Subsequent to this step, 5µl each of Annexin V-FITC and PI were introduced into the cell suspension. The solutions underwent gentle agitation and were then subjected to an incubation period lasting 15 min, all while maintaining room temperature and darkness. Concurrently, a set of control samples was also prepared. A BD FACS Calibur Flow Cytometer was employed to quantify early apoptotic cells, marked by Annexin V-FITC positivity, and late apoptotic or necrotic cells, identified by dual positivity for Annexin V-FITC and PI.

Western blot

Protein extraction from A549 cells treated with HCQ at predetermined concentrations was conducted, and their concentrations were assessed via a BCA protein assay kit. In the process of conducting western blot analysis, an equivalent quantity of protein, specifically 20µg, was first segregated using SDS-PAGE technique which were transferred onto PVDF membranes. Following a wash with Tris-Buffered Saline (TBS), the membranes were incubated in a solution of 5% skim milk in TBS for 1h under normal conditions to block nonspecific binding. Subsequent to this blocking step, the membranes were subjected to incubation with specific primary antibodies targeting various proteins, including GAPDH (1:2500), and the following at a dilution of 1:1000: cyclin E1, CDK2 cyclin D1, CDK4, p21, Bcl-2, Bax, cytochrome C, caspase-3, PARP, p-JNK, JNK, p-STAT3, STAT3, p-AKT, AKT, p53. The incubation process was carried out overnight, maintaining the samples at a constant temperature of 4°C throughout the entire duration. Afterward, the membranes were exposed to anti-rabbit IgG conjugated with Horse Radish Peroxidase (HRP). Ultimately, visualization of the reactive bands was facilitated through the utilization of an enhanced Chemiluminescent Substrate tailored for HRP detection. GAPDH was used as loading control.

Nude mouse xenograft model

BALB/c nude mice, at an age range of 5 to 6 weeks, which originated from Liaoning Changsheng Biotechnology Co., Ltd. Animal protocols underwent approval from the Animal Ethical Care Committee of Qiqihar Medical University (Approval Number: QMU-AECC-2022-50). Establishing the xenograft model involved the subcutaneous injection of 2×10^6 A549 cells into the flanks of BALB/c mice devoid of fur at the age of five weeks. Once tumor volumes averaged 50 mm^3, 10 mice with tumors were subjected to random allocation into either the HCQ-treated group or the control group (n=5 mice per group). Mice in the HCQ-treated and control groups were injected with equal doses of HCQ (mg/kg) and Phosphate-Buffered Saline (PBS), respectively. On the 21st day after administration, the tumors were harvested, weighed and photographed.

STATISTICAL ANALYSIS

The experiments were carried out independently, each repeated no less than three times, with triplicates per

experimental point to ensure robustness and reliability of the results. Data obtained in this experiment were expressed as the mean accompanied by ± SD, providing a measure of both central tendency and variability within the data set. Statistical analysis involved the utilization of ANOVA, which was further complemented by a Student's t-test. A *p*-value below 0.05 was considered to suggest statistical significance, guiding the interpretation of experimental outcomes.

RESULTS

HCQ inhibited the cell growth of A549 cells in vitro and in vivo

The effects of HCQ on A549 cells *in vitro* and *in vivo* were investigated. Initially, A549 cells were subjected to various concentrations of HCQ for a full day or two respectively, subsequently assessment of cell viability utilizing the MTT assay. fig. 2 illustrates that HCQ treatment led to an inhibition of A549 cell survival that varies with dose and duration. Notably, significant decreases in cell viability were observed at concentration of 60μM after 24h (($p<0.01$) or 30μM after 48h ($p<0.05$), indicating substantial efficacy. The peak inhibition (89.3%) was reached using an HCQ concentration of 150μM in 48h. Furthermore, the IC_{50} values were calculated for different time points. Over the course of 24h, the IC_{50} value was found to be 78.6μM, in contrast, after 48 hours, the IC_{50} value decreased to 58.6 μM, demonstrated the potency of HCQ in inhibiting A549 cell growth. Moreover, HCQ treatment demonstrated efficacy in controlling xenograft tumors. As depicted in fig. 3, the weight of xenotumors were markedly lower in the HCQ treatment group in comparison with the control group. This significant reduction suggests that HCQ strongly suppresses tumor growth *in vivo*.

HCQ inhibited the growth of A549 cells by suppressing the phosphorylation of JNK, STAT3 and AKT

The activation of JNK, STAT3 and AKT signals seems to be very important for tumor cell growth and formation in some physiological and pathological contexts. To investigate the signaling mechanisms underlying HCQ-induced growth inhibition, the phosphorylation levels of JNK, STAT3 were measured in A549 cells using western blot analysis, while AKT presence was detected, both with and without HCQ treatment. In A549 cells treated with HCQ, there was a dose-dependent decrease observed in the phosphorylation levels of JNK, STATs and AKT, in contrast to the control group. Although JNK's overall expression levers STAT3 and AKT remained unchanged (see fig. 4). These findings suggest that the inactivation of JNK, STAT3 and AKT signals are participating in the growth inhibition impact of HCQ on A549 cells.

HCQ induced Gap 1 (G1) arrest by modulating cell cycle-associated proteins in A549 cells

To investigate the relationship between cell cycle arrest and HCQ-mediated inhibition of A549 cell growth, flow cytometry was employed for cell cycle analysis. The findings demonstrated that with escalating concentrations of HCQ the proportion of cells in the G1 phase rose by 15.88%, from 62.06% to 77.94%, while the proportion of cells in the S phase declined by 12.56%, from 30.73% to 18.17%. Nevertheless, no noticeable alteration was detected in the quantity of cells in the G2 phase. In light of these discoveries, the evidence presented bolsters the proposition that HCQ prompts G1 phase cell cycle arrest specifically within A549 cells (see fig. 5).

The cell cycle is motivated by activation of CDKs, which are under the positive regulation of cyclin and the negative regulation of CDK inhibitors (CDKIs). p53, as a tumor suppressor gene, is reported that can up-regulate p21 expression. Subsequently, p21 combines with cyclin E-CDK2 and cyclin D-CDK4, leading to the arrest of cells in the G1 phase. As depicted in fig. 6, HCQ treatment markedly elevated the expression levels of both p53 and p21, while reducing the levels of CDK2, CDK4, cyclin E1 and cyclin D1 in contrast to the control cohort. Additionally, this impact was dose-dependent. It is speculated that HCQ treatment induced the expression levels of both p53 and p21, which further impaired the activity of cyclins and CDKs. This directly induces A549 cell cycle arrest in G1 phase and further inhibits A549 cell growth.

HCQ induces mitochondrial-mediated apoptosis in A549 cells

Beside cell cycle arrest, apoptosis induced by HCQ was the main mechanism of A549 cell growth inhibition. AO/EB staining further explored whether HCQ-induced growth inhibition via cell apoptosis. Following 24 h of exposure to HCQ, there was an observable alteration in the morphology of A549 cells. As fig. 7A illustrates, A549 cells exposed to HCQ showed typical morphological characteristics of apoptosis. Apoptosis induction in A549 cells was further confirmed by Annexin V-FITC/PI assay. As fig. 7B illustrates, HCQ treatment led to an augmentation of early apoptotic cells in a manner dependent on concentration. Early apoptotic cell proportion rose significantly from 3.61% of untreated cells to 6.46%, 10.80%, 15.55% respectively in 30, 60, 90 μM HCQ-treated cells for 24 h. However, whether treated with HCQ or not, no significant change detected in the quantity of late apoptotic cells.

It is recognized that protein families called Bcl-2 and caspases are usually activated in the early stage of apoptosis. p53, as a transcriptional promoter, regulates the expression of many proteins required for cell apoptosis including Bax and Bcl-2. It is reported that p53 can directly activate pro-apoptotic factor Bax, make mitochondria permeable and induce apoptosis. Specifically, the proteins examined included Bcl-2, Bax, cytochrome C, c-Caspase-3 and c-PARP.

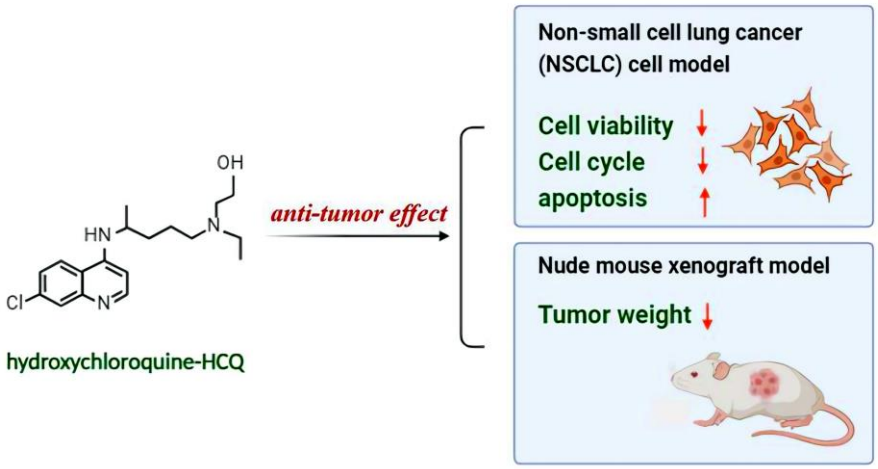

Fig. 1: Infographic showed Hydroxychloroquine (HCQ) effectively inhibited A549 cell growth *in vitro* as well as *in vivo*.

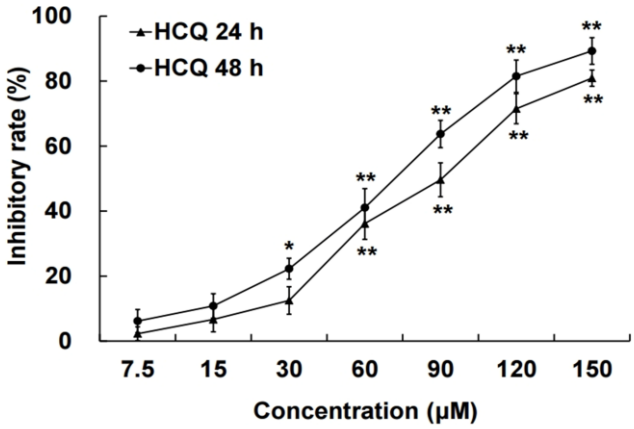

Fig. 2: HCQ inhibited cell viability in human A549 cells. Human A549 cells were seeded into 96-well plates (5×10^3 cells/well) and treated with or without the indicated concentrations of HCQ for 24 or 48 h, respectively. Cell viability was determined by MTT assay, followed by calculating the inhibition rates. Data are presented as the mean ± SD of each group from three independent triplicate experiments. *p<0.05 and **p<0.01 compared with the control group.

Fig. 3: HCQ treatment inhibited the growth of xenograft tumor growth in mice. Nude Mouse Xenograft Model was established by subcutaneously injecting 2×10^6 A549 cells into the flanks of 5-week-old nude BALB/c mice. Tumor size and weight were monitored on the 21st day after administration.

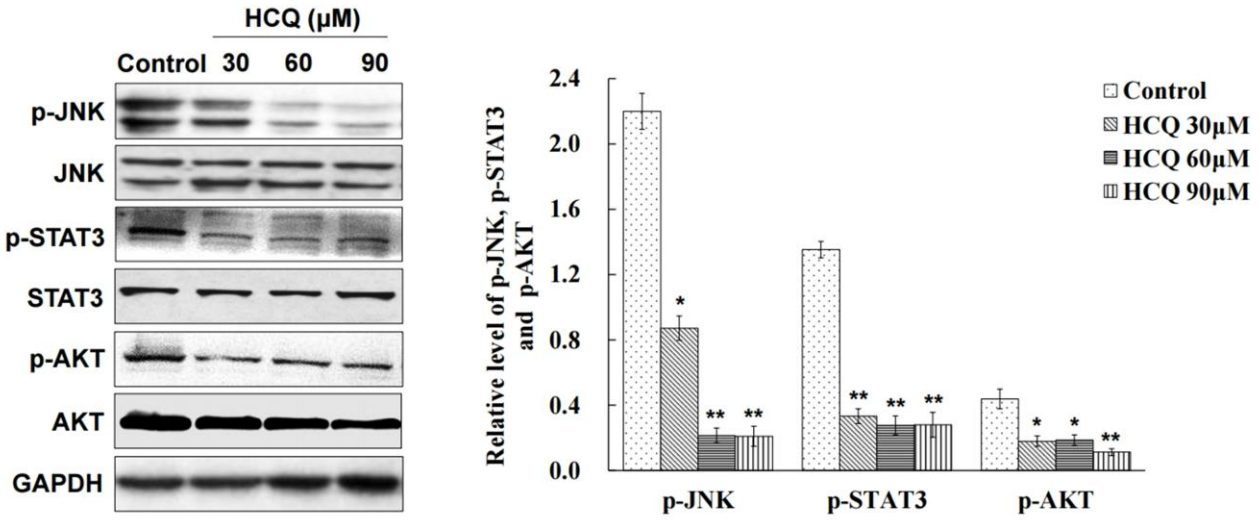

Fig. 4: Inactivation of JNK, STAT3 and AKT associated with HCQ-induced growth inhibition in A549 cells. Cells were treated with varying concentrations of HCQ (0, 30, 60, 90μM) for 24h and protein levels of phosphorylated JNK (p-JNK), phosphorylated STAT3 (p-STAT3) and phosphorylated AKT (p-AKT) were determined by western blot analysis. GAPDH was utilized as a loading control. Data are presented as the mean ± SD of three independent experiments. *p<0.05 and **p<0.01 compared with the control group.

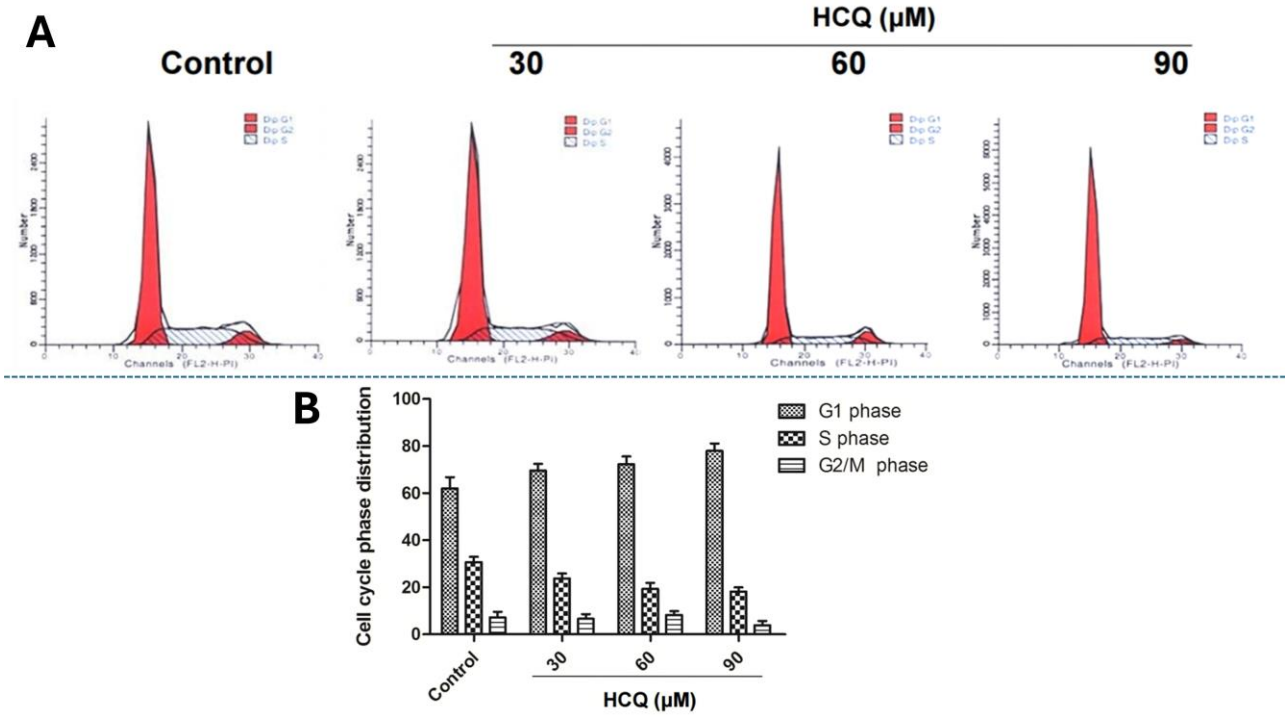

Fig. 5: HCQ induced G1 cell cycle arrest in A549 cells. (A) Distribution of cells in G1, S or G2 phase in A549 cells following treatment with HCQ at concentrations of 30, 60 and 90μM or without treatment for 24h; (B) Percentage of cell population in the G1, S and G2 phase.

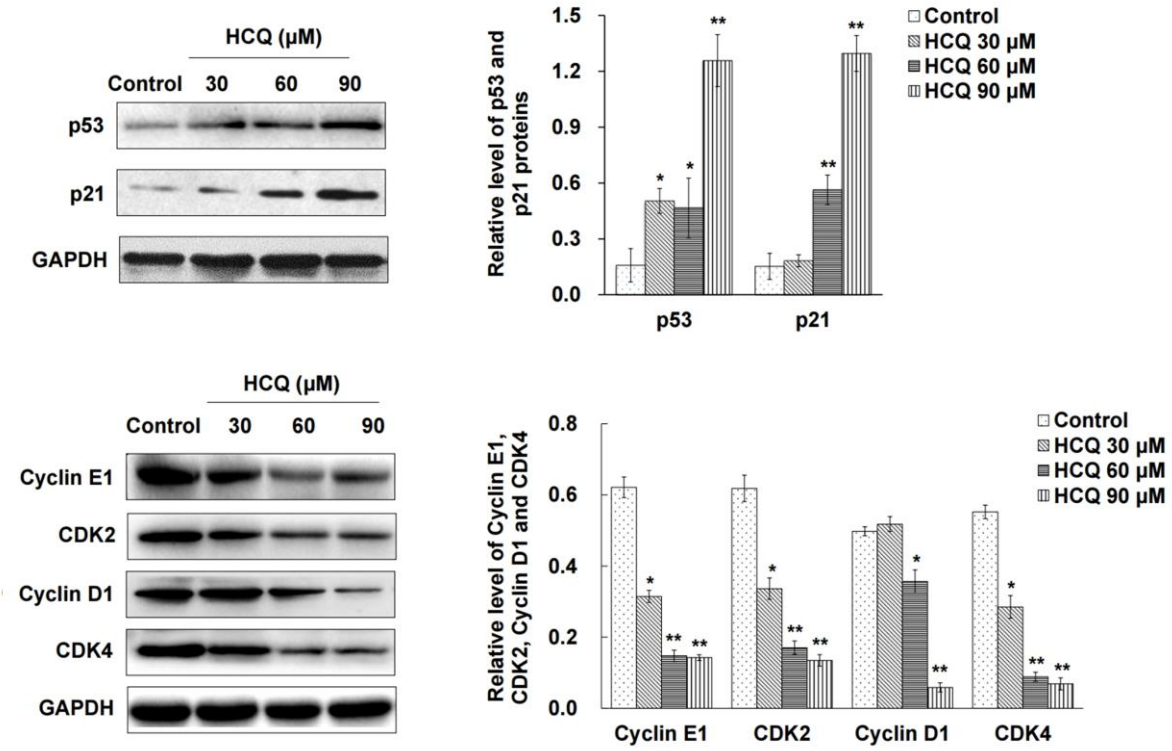

Fig. 6: HCQ regulated the expression of cell-cycle related proteins in A549 cells. Cells were treated with HCQ at different concentrations (0, 30, 60, 90μM) for 24h. Protein levels of cyclin E1, CDK2, cyclin D1, CDK4, p21 and p53 were determined by western blot analysis. GAPDH was used as a loading control. Data are presented as the mean ± SD of three independent experiments. *p<0.05 and **p<0.01 compared with the control group.

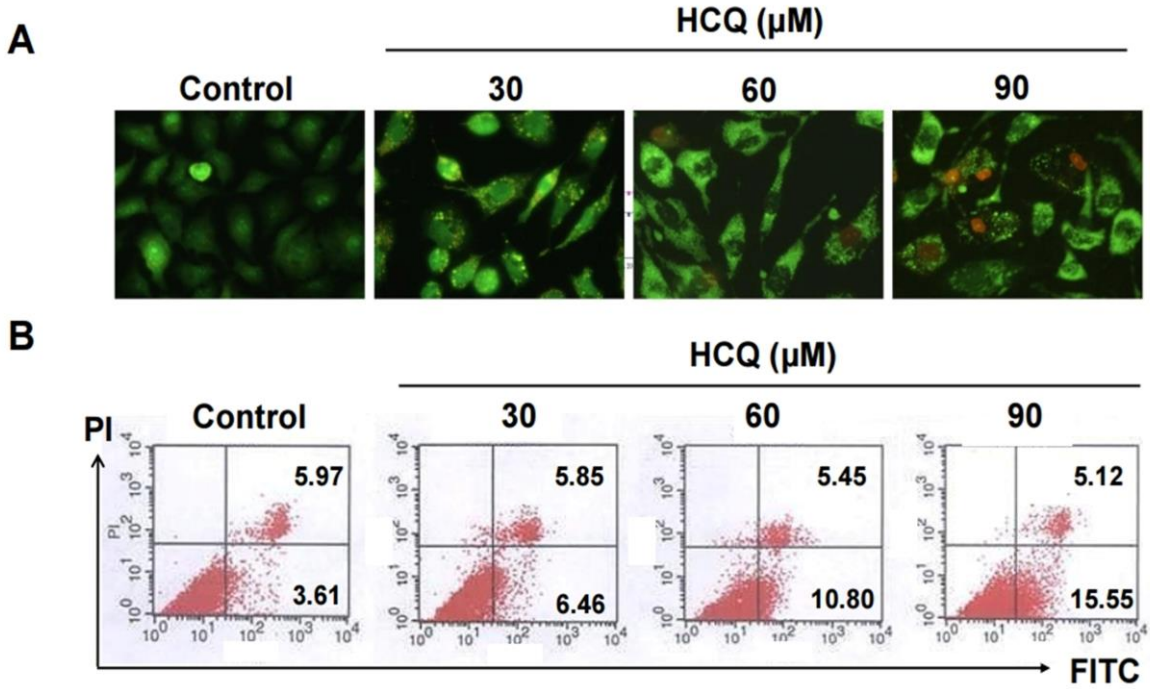

Fig. 7: HCQ induced early stage apoptosis in A549 cells. (A) Cells were treated with HCQ at different concentrations (0, 30, 60, 90μM) for 24h, stained with acridine orange/ethidium bromide (AO/EB) and then observed under fluorescence microscopy. Green fluorescence indicated normal and early apoptotic cells, while late apoptotic cells exhibited red-orange fluorescence in the nucleus. (B) A scattergram of apoptotic A549 cells stained with Annexin V and propidium iodide (PI) analyzed by flow cytometry.

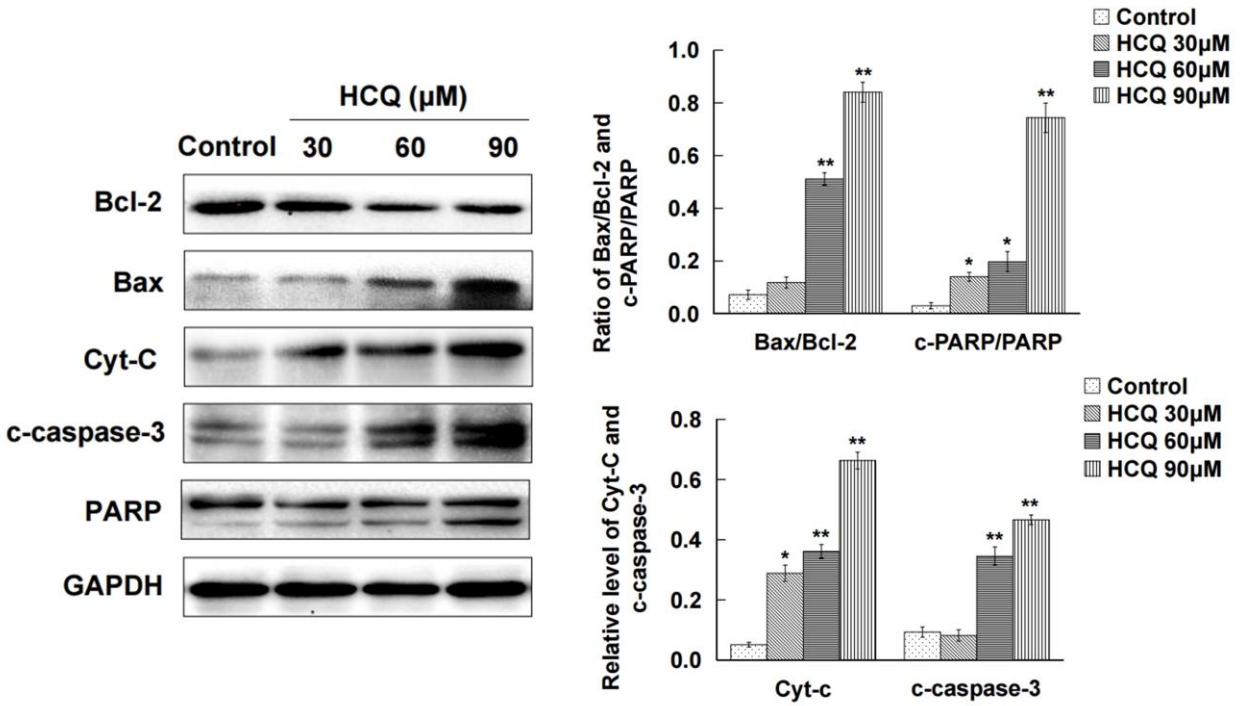

Fig. 8: HCQ induced apoptosis of A549 cells via mitochondrial signaling pathway. Cells were treated with HCQ at different concentrations (0, 30, 60, 90μM) for 24h and protein levels of Bcl-2, Bax, cytochrome C (Cyt-C), cleaved caspase-3 (c-caspase-3) and PARP were determined by western blot analysis. GAPDH served as the loading control. Data are presented as the mean ± SD of three independent experiments. *p<0.05 and **p<0.01 compared with the control group.

As shown in fig. 8, HCQ-treated cells exhibited a dose-dependent upregulation of Bax, cytochrome C, c-Caspase-3 and c-PARP, accompanied by a down regulation of Bcl-2. We speculated that HCQ treatment activates p53 expression, further increases Bax expression, reduces Bcl-2 expression and results in a rise in the Bax/Bcl-2 ratio. The imbalance between Bax and Bcl-2 triggers the translocation of cytochrome C from mitochondria to the cytosol, initiating the activation of caspase-3 and the cleavage of PARP, ultimately culminating in apoptosis. In summary, our findings confirmed that HCQ treatment elevates p53 expression, thereby instigating mitochondrial-dependent apoptosis.

DISCUSSION

HCQ, a hydroxylated analogue of CQ, has been developed to treat malaria and autoimmune diseases and has similar efficacy but lower toxicity compared with CQ (Hoekenga, 1955). Recently, HCQ has been studied as an effective anticancer drug. Demonstrated evidence indicates that HCQ can increase tumor cell death alone or in conjunction with chemotherapy or radiotherapy (Solomon, Lee, 2009). However, until now, not much is understood about the process by which HCQ displayed antitumor activity in NSCLC. Herein, it was found that HCQ effectively inhibited A549 cell proliferation *in vitro* as well as *in vivo*. This growth inhibition is mainly achieved by inhibiting phosphorylation of JNK, STAT3 and AKT, subsequently causing A549 cells to undergo mitochondrial-mediated apoptosis and G1 cell cycle arrest as a result.

JNK, a well-studied kinase controlling cell growth, is primarily associated with proapoptotic cell death (Nadel, Maik-Rachline, Aeger, 2023). It is quite important in modulating the activities of pro- and anti-apoptotic proteins within mitochondria, thereby initiating apoptosis. STAT3, functioning as a cytoplasmic transcription factor, forms dimer upon activation, swiftly forming dimers and translocating from the cytoplasm into the nucleus. This migration facilitates the induction of downstream gene transcription, which is integral to processes like survival, apoptosis and so on (Mohassab *et al.*, 2020; Wang *et al.*, 2023). The AKT signaling cascade, a crucial signaling pathway in eukaryotic cells, regulates multiple cellular processes. Demonstration has been made that the inhibition of AKT suppresses cell proliferation and induces apoptosis in diverse cancer cell lines (Song *et al.*, 2019; Kim, You, Youn, 2022; Chen *et al.*, 2022). This study proves that JNK, STAT3 and AKT were a primary focus and that the total levels of the proteins in this trial remained constant. This finding unequivocally validates the association between growth inhibition observed in A549 cells exposed to HCQ and the inhibition of JNK, STAT3 and AKT signaling pathways.

The regulation of the course of the cell cycle is very important for determining the fate of cells. It encompasses a delicate balance of signals and checkpoints, ensuring the accurate progression of each stage. In eukaryotic cells, there are four unique stages in the cell cycle, which include G1 phase, Synthesis (S) phase, Gap 2 (G2) phase and Mitosis (M) phase (Vermeulen, Berneman, Van Bockstaele, 2003). Each phase seamlessly transitions into the next, orchestrating the precise replication and division necessary for cellular function and proliferation. The G1/S transition is known to be a key regulatory point in the cell cycle where cells decide whether they should proliferate, undergo apoptosis or entry a state of quiescence (Otto, Sicinski, 2017). The current study demonstrated that treatment with HCQ led to alterations in the distribution of A549 cells. Within eukaryotic organisms, the cell cycle operates under meticulous regulation, orchestrated by a sophisticated mechanism that encompasses a multitude of protein kinases, including CDKs coupled with their respective cyclin regulatory subunits, alongside CDKIs. The cyclin D-CDK4 and cyclin E-CDK2 predominantly function in regulating the G1/S transition of the cell cycle. They actively regulate this progression by phosphorylating specific target proteins and drive cell cycle progression. The complexes' activity can be negatively regulated by CDKIs such as p21 (Sherr, 1996). Studies has shown that p21 can directly bind to cyclin-CDK complexes, disrupting their ability to phosphorylate target proteins involved (Shamloo, Usluer, 2019). To clarify the molecular mechanisms involved, we analyzed the relative expression levels of cyclin E1, CDK2, cyclin D1, CDK4 and p21 expression in A549 cells treated with HCQ. Our findings revealed a notable rise in p21 level and a notable rise in the expression of cyclin E1, cyclin D1, CDK2 and CDK4 upon HCQ treatment with varying concentrations. These findings imply that HCQ treatment able to boost p21 expression, thus inhibiting the activity of cyclin E1-CDK2 and cyclin D1-CDK4 complex and finally leading to G1 phase arrest. P53 is widely regarded as a regulator factor in cell cycle. It is reported that activated p53 causes a G1 phase cell cycle arrest made by regulating the expression of p21 which directly bind to cyclin/CDK complex to inhibit its activity (Luo *et al*., 2022). We conducted a study to the potential involvement of p53 in the G1 arrest of A549 cells induced by HCQ. The findings from the study show that with increasing doses of HCQ, there was a corresponding dose-dependent rise observed in the expression levels of p53. In light of these observations, we posit that HCQ treatment activates p53, leading to the upregulation of p21 expression. Subsequently, elevated p21 levels inhibit the activities of cyclin E1/CDK2 and cyclin D1-CDK4 complexes, thereby causing cell cycle arrest in A549 cells at the G1 phase.

Cell apoptosis and proliferation are tightly interwined processes. Both the halting of cell cycle progression and the induction of apoptosis can be brought on by identical stimuli. Certain proteins, such as p53, are common to the cell cycle and apoptosis, providing a rationale for their correlation (Wang, 2023). The induction of apoptosis is commonly attributed to p53. Research has revealed that p53 participated in apoptosis induction by regulating both anti-apoptotic and pro-apoptotic factors, leading to the mitochondria's release of Bax/Bak, subsequent cytochrome C release and activation of procaspase-3 (Pistritto *et al*., 2016; hao, 2023). In this study, an additional endeavor was made to delineate the mechanism underlying HCQ's effects in A549 cells. Protein levels related to apoptosis Protein levels related to apoptosis that HCQ treatment decreased the levels of Bcl-2 and PARP, but interestingly, improved the expression in which Bax, cytochrome C and cleaved caspase-3. The evidence suggests that HCQ initiates a cascade of events culminating in mitochondrial-mediated apoptosis. This process involves the down regulation of Bcl-2 expression and the concurrent up regulation of Bax levels. As a result, cytochrome C moves from mitochondria to the cytosol, initiating a caspase cascade. Ultimately, this leads to the activation of caspase-3 and the cleavage of PARP, thus driving the apoptotic process forward.

CONCLUSION

To sum up, our investigation uncovered that the proliferation of A549 cells is notably restrained by the actions of HCQ. This effect is achieved through the induction of cell cycle arrest and the promotion of apoptosis. These effects may be partially attributed to the inhibitory effect of HCQ on the JNK, STATs, and AKT signaling pathways. In animal models, HCQ significantly inhibited the growth of NSCLC tumors. Therefore, these results from this study offer robust evidence endorsing the prospective utilization of HCQ for managing NSCLC, and the foundation for further exploration of its mechanisms of action and clinical applications.

Nonetheless, it is crucial to recognize that this study is not without its limitations. It is essential to consider these constraints when interpreting the findings. To begin with, our investigations were primarily conducted in A549 cells and a xenograft mouse model, which may not fully represent the complexity of NSCLC in clinical settings. Additionally, while we identified several key molecular pathways involved, further elucidation of the precise mechanisms and potential off-target effects of HCQ is warranted. For future research, it would be beneficial to explore the efficacy of HCQ in other NSCLC cell lines and animal models to validate its therapeutic potential across diverse contexts. Furthermore, investigating potential combination therapies involving HCQ with existing anti-cancer agents could enhance its effectiveness and minimize resistance development. Lastly, it is imperative that clinical trials be conducted to conduct a

comprehensive evaluation of both the safety and effectiveness of HCQ as a potential treatment option for patients with NSCLC. Such evaluations are essential to determine its suitability and effectiveness in a clinical setting.

ACKNOWLEDGMENTS

The authors wish to extend their gratitude to Li Zhou and Li Fan who come from Research Institute of Medicine and Pharmacy of Qiqihar Medical University. Their technical assistance has been invaluable. Additionally, this research received funding support from the Natural Science Foundation of Heilongjiang Province (LH2022H108), the Education Department Foundation of Heilongjiang Province (2021-KYYWF-0337) and the Key Cultivation Project of Qiqihar Medical University (2021-ZDPY-010).

CONFLICT OF INTEREST

It is officially verified that all authors involved in this study declare no personal or financial conflicts of interest that might have impacted the results or interpretations presented in this work.

REFERENCES

Bhatt V, Lan T, Wang W, Kong J, Lopes EC, Wang J, Khayati K, Raju A, Rangel M, Lopez E, Hu ZS, Luo X, Su X, Malhotra J, Hu W, Pine SR, White E and Guo JY (2023). Inhibition of autophagy and MEK promotes ferroptosis in Lkb1-deficient Kras-driven lung tumors. *Cell Death Dis.*, **14**(1): 61-74.

Bray F, Laversanne M, Sung H, Ferlay J, Siegel RL, Soerjomataram I and Jemal A (2024). Global cancer statistics 2022: GLOBOCAN estimates of incidence and mortality worldwide for 36 cancers in 185 countries. *CA Cancer J. Clin.*, **74**(3): 229-263.

Chen J, Pan Q, Bai Y, Chen X and Zhou Y (2021). Hydroxychloroquine induces apoptosis in cholangiocarcinoma via reactive oxygen species accumulation induced by autophagy inhibition. *Front. Mol. Biosci.*, **8**: 720370.

Chen MC, Annseles Rajula S, Bharath Kumar V, Hsu CH, Day CH, Chen RJ, Wang TF, Viswanadha VP, Li CC and Huang CY (2022). Tannic acid attenuate AKT phosphorylation to inhibit UMUC3 bladder cancer cell proliferation. *Mol. Cell Biochem.*, **477**(12): 2863-2869.

Chou KY, Chen PC, Chang AC, Tsai TF, Chen HE, Ho CY and Hwang TI (2021). Attenuation of chloroquine and hydroxychloroquine on the invasive potential of bladder cancer through targeting matrix metalloproteinase 2 expression. *Environ. Toxicol.*, **36**(11): 2138-2145.

Fong W and To KKW (2021). Repurposing chloroquine analogs as an adjuvant cancer therapy. *Recent Pat. Anticancer Drug Discov.*, **16**(2): 204-221.

Guo H, Zhang J, Qin C, Yan H, Liu T, Hu H, Tang S, Tang S and Zhou H (2022). Biomarker-targeted therapies in non-small cell lung cancer: Current status and perspectives. *Cells*, **11**(20): 3200-3223.

Hao Q, Chen J, Lu H and Zhou X (2023). The ARTS of p53-dependent mitochondrial apoptosis. *J. Mol. Cell Biol.*, **14**(10): mjac074.

Herbst RS, Morgensztern D and Boshoff C (2018). The biology and management of non-small cell lung cancer. *Nature*, **553**(7689): 446-454.

Hoekenga MT (1955). The treatment of malaria with hydroxychloroquine. *Am. J. Trop Med. Hyg.*, **4**(2): 221-223.

Johnson DE, O'Keefe RA and Grandis JR (2018). Targeting the IL-6/JAK/STAT3 signalling axis in cancer. *Nat. Rev. Clin. Oncol.*, **15**(4): 234-248.

Kim J, You HJ and Youn C (2022). SCARA3 inhibits cell proliferation and EMT through AKT signaling pathway in lung cancer. *BMC Cancer*, **22**(1): 552-564.

Lagneaux L, Delforge A, Carlier S, Massy M, Bernier M and Bron D (2001). Early induction of apoptosis in B-chronic lymphocytic leukaemia cells by hydroxychloroquine: activation of caspase-3 and no protection by survival factors. *Br. J. Haematol.*, **112**(2): 344-352.

Lagneaux L, Delforge A, Dejeneffe M, Massy M, Bernier M and Bron D (2002). Hydroxychloroquine-induced apoptosis of chronic lymphocytic leukemia involves activation of caspase-3 and modulation of Bcl-2/bax/ratio. *Leuk Lymphoma.*, **43**(5): 1087-1095.

Li Y, Cao F, Li M, Li P, Yu Y, Xiang L, Xu T, Lei J, Tai YY, Zhu J, Yang B, Jiang Y, Zhang X, Duo L, Chen P and Yu X (2018). Hydroxychloroquine induced lung cancer suppression by enhancing chemo-sensitization and promoting the transition of M2-TAMs to M1-like macrophages. *J. Exp. Clin. Cancer Res.*, **37**(1): 259-274.

Liu LQ, Wang SB, Shao YF, Shi JN, Wang W, Chen WY, Ye ZQ, Jiang JY, Fang QX, Zhang GB and Xuan ZX (2019). Hydroxychloroquine potentiates the anti-cancer effect of bevacizumab on glioblastoma via the inhibition of autophagy. *Biomed. Pharmacother.*, **118**: 109339.

Luo D, Yu C, Yu J, Su C, Li S and Liang P (2022). p53-mediated G1 arrest requires the induction of both p21 and Killin in human colon cancer cells. *Cell Cycle*, **21**(2): 140-151.

Miller KD, Nogueira L, Devasia T, Mariotto AB, Yabroff KR, Jemal A, Kramer J and Siegel RL (2022). Cancer treatment and survivorship statistics, *CA Cancer J. Clin.*, **72**(5): 409-436.

Mohassab AM, Hassan HA, Abdelhamid D, Abdel-Aziz M (2020). STAT3 transcription factor as target for anti-cancer therapy. *Pharmacol. Rep.*, **72**(5): 1101-1124.

Nadel G, Maik-Rachline G and Seger R (2023). JNK cascade-induced apoptosis-a unique role in gqpcr

signaling. *Int. J. Mol. Sci.*, **24**(17): 13527-13544.
Nirk EL, Reggiori F and Mauthe M (2020). Hydroxychloroquine in rheumatic autoimmune disorders and beyond. *EMBO Mol. Med.*, **12**(8): e12476.
Otto T and Sicinski P (2017). Cell cycle proteins as promising targets in cancer therapy. *Nat. Rev. Cancer*, **17**(2): 93-115.
Peng X, Zhang S, Jiao W, Zhong Z, Yang Y, Claret FX, Elkabets M, Wang F, Wang R, Zhong Y, Chen ZS and Kong D (2021). Hydroxychloroquine synergizes with the PI3K inhibitor BKM120 to exhibit antitumor efficacy independent of autophagy. *J. Exp. Clin. Cancer Res.*, **40**(1): 374-394.
Pistritto G, Trisciuoglio D, Ceci C, Garufi A and D'Orazi G (2016). Apoptosis as anticancer mechanism: Function and dysfunction of its modulators and targeted therapeutic strategies. *Aging (Albany NY)*, **8**(4): 603-619.
Ponticelli C, Moroni G (2017). Hydroxychloroquine in systemic lupus erythematosus (SLE). *Expert Opin. Drug Saf.*, **16**(3): 411-419.
Rahim R and Strobl JS (2009). Hydroxychloroquine, chloroquine, and all-trans retinoic acid regulate growth, survival, and histone acetylation in breast cancer cells. *Anticancer Drugs*, **20**(8): 736-745.
Shamloo B and Usluer S (2019). p21 in Cancer Research. *Cancers (Basel)*, **11**(8): 1178.
Sherr CJ (1996). Cancer cell cycles. *Science*, **274**(5293): 1672-1677.
Solomon VR, Lee H (2009). Chloroquine and its analogs: a new promise of an old drug for effective and safe cancer therapies. *Eur. J. Pharmacol.*, **625**(1-3): 220-233.
Song M, Bode AM, Dong Z and Lee MH (2019). AKT as a therapeutic target for cancer. *Cancer Res.*, **79**(6): 1019-1031.
Vermeulen K, Berneman ZN and Van Bockstaele DR (2003). Cell cycle and apoptosis. *Cell Prolif.*, **36**(3): 165-175.
Wang H, Guo M, Wei H and Chen Y (2023). Targeting p53 pathways: Mechanisms, structures and advances in therapy. *Signal Transduct Target Ther.*, **8**(1): 92-126.
Wang W, Lopez McDonald MC, Kim C, Ma M, Pan ZT, Kaufmann C and Frank DA (2023). The complementary roles of STAT3 and STAT1 in cancer biology: Insights into tumor pathogenesis and therapeutic strategies. *Front Immunol.*, **14**: 1265818.